ChemPubSoc Europe

DOI: 10.1002/open.201700196

Open Access ChemistryOPEN Communications

Regiochemical Control in Triptycene Formation—An Exercise in Subtle Balancing Multiple Factors

Jan-Hendrik Lamm, Yury V. Vishnevskiy, Eric Ziemann, Beate Neumann, Hans-Georg Stammler, and Norbert W. Mitzel*[a]

Reactions between 1,8-dichloroanthracenes with substituents in position 10 and *ortho*-chloroaryne afford mixtures of 1,8,13- (*syn*) and 1,8,16-trichlorotriptycenes (*anti*). The *syn*/*anti* ratio is dependent on these substituents. Electropositive substituents like $SiMe_3$ and $GeMe_3$ lead to preferred formation of the *syn*-isomer, whereas CMe_3 groups exclusively afford the *anti*-isomer. Different quantum chemical calculations including location of transition states give conflicting results, but indicate the importance of dispersion forces for an at least qualitative prediction of results. The *syn*-trichlorotriptycenes with $SiMe_3$ and $GeMe_3$ substituents were characterized by using NMR spectroscopy, mass spectrometry, and X-ray diffraction experiments.

Triptycene represents one of a few rigid organic frameworks of D_{3h} symmetry without any (Lewis-basic) heteroatoms. It was first synthesized by Bartlett et al. in 1942 using a multi-step procedure starting from anthracene and *p*-benzoquinone.[1] In 1956, Wittig and Ludwig reported a more efficient access to triptycene in one step from anthracene by reacting it with in situ-formed benzyne.[2] The symmetry and rigidity of triptycene have inspired a plethora of applications in fundamental and applied chemical research.[3–5] Substituted triptycenes are widely used, for example, as building blocks for fluorescent or non-fluorescent organic macromolecules, polymers, and liquid crystals,[3,6] as rigid spacers in several Pd complexes used for cross coupling reactions,[7] as devices in molecular machines,[8] in crystal engineering processes,[9,10] and as a basis for the design of highly porous organic materials with numerous applications.[11]

[a] *Dr. J.-H. Lamm, Dr. Yu. V. Vishnevskiy, E. Ziemann, B. Neumann, Dr. H.-G. Stammler, Prof. Dr. N. W. Mitzel*
Lehrstuhl für Anorganische Chemie und Strukturchemie
Centrum für Molekulare Materialien CM_2
Universität Bielefeld, Fakultät für Chemie
Universitätsstraße 25, 33615 Bielefeld (Germany)
Fax: (+49)521 106—6026
www.uni-bielefeld.de/chemie/arbeitsbereiche/ac3-mitzel/
E-mail: mitzel@uni-bielefeld.de

Supporting Information and the ORCID identification number(s) for the author(s) of this article can be found under https://doi.org/10.1002/open.201700196.

Although the chemistry of triptycenes and their functionalization is generally in an advanced state, the 1,8,13-trisubstitution motif remains a challenge for synthesis. However, exactly this pattern is interesting to introduce three functionalities oriented in the same direction. We try to make use of such 1,8,13-trisubstituted triptycenes (also called *syn*-triptycenes) as rigid organic frameworks for constructing directed polydentate Lewis acids,[12,13] but many other applications might be envisioned.

syn-Triptycenes can be obtained through Diels–Alder reactions of 1,8-disubstituted anthracenes with *ortho*-functionalized arynes, a protocol introduced by Rogers and Averill in 1986.[14] The drawback of this method is that the corresponding *anti*-trisubstituted 1,8,16-isomer is always formed as the main product when, for example, Cl-functionalized anthracenes and arynes are used.[12,14] In 2010, we reported attempts to increase the *syn*/*anti* ratio by making use of the steric interference of the (bulky) anthracene substituent at C-10 with the chlorine atom of the chloroaryne (Scheme 1). We expected this strategy to

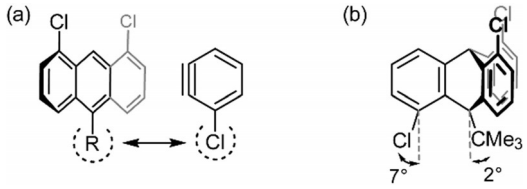

Scheme 1. a) Proposed steric interactions of 10-substituted 1,8-dichloroanthracenes and chloroaryne; b) structural data for a *tert*-butyl derivative.

provide an increased formation of the *syn*-isomer. However, the steric influence of the C-10 substituent turned out to be minimal, whereas the electronic properties are dominant;[12] of all substituents tested, the biggest $R=C(CH_3)_3$ led to the formation of 100% *anti*-isomer, despite the formation of an extremely deformed product by mutual repulsion of the Cl and R substituents, as indicated in Scheme 1b.

Accepting that we cannot take steric control over this reaction, it is necessary to understand the electronic parameters determining it. Cycloadditions of substituted arynes have been studied experimentally and theoretically. Their reactions have been predicted by steric, charge-controlled, and aryne-distortion models; the latter two have recently been given preference and predict nucleophilic attack to be preferred at C-3 in 3-chlorobenzyne.[15]

First, simple DFT calculations [B3LYP/6-31G(d,p)] indicated that the charge distribution of the carbon skeletons of the anthracene and benzyne can be manipulated by different sub-

stituents. However, the predicted partial charges depend very much on the quantum-chemical method employed. Although in a recent theoretical study the charge distribution of chlorobenzyne has been given as +0.11 (C-2) and −0.04 *e* (C-3) [NBO charges, B3LYP/6–311+G(d,p)],[15] we find contradictory results between natural bond orbital (NBO)[16] (C2−0.02, C3+0.10 *e*) and atoms in molecules (AIM)[17] (C-2+0.01, C-3−0.21 *e*) charges (B3LYP/6-31G(d,p) [further details can be found in the Supporting Information, and electrostatic potentials (ESP) are also reported therein]. This demonstrates that the charge argument is less clear-cut than suggested. More unambiguous are charges predicted for a range of 10-substituted anthracene molecules: although the charge at C-9 is virtually invariant for all molecules (R = $SiMe_3$, CMe_3, Ph, Cy, *i*Pr, Me, H) (NBO −0.18 to −0.17, AIM +0.01 *e* for all), the charge at C-10 is clearly more negative (NBO −0.44, AIM −0.65 *e*) for R = $SiMe_3$ than for all carbon substituents (NBO +0.03 to +0.04, AIM 0 to −0.02 *e*). This distinction is clear, such that a $SiMe_3$ group was likely to exert the desired regiochemical effect.

The limited number of available electropositive functions compatible with the other reactive groups in the systems restricts the choice of possibilities. However, 1,8-dichloroanthracenes with EMe_3 (E = Si, Ge) substituents in position 10 were accessible from earlier projects: 10-bromo-1,8-dichloroanthracene can selectively be metalated with *n*BuLi and the carbanion reacted with Me_3ECl reagents.[18] The 10-EMe_3-1,8-dichloroanthracenes with E = Si (**1**) and Ge (**2**) were then reacted with in situ-generated chloroaryne to obtain the corresponding trichlorotriptycenes (Scheme 2), which were then used to test the validity of the predictions.

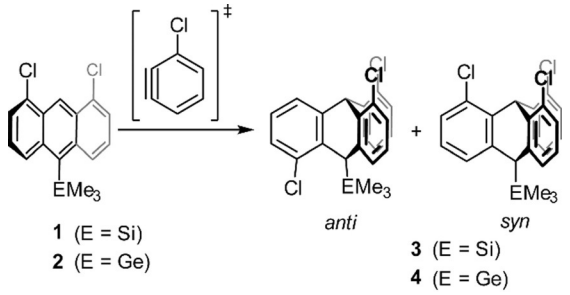

Scheme 2. Conversion of the 10-trimethylelement-substituted 1,8-dichloroanthracenes **1** and **2** with in situ-generated chloroaryne to afford the trichlorotriptycenes **3** and **4**. Reagents and conditions: 1) 3-chloroanthranilic acid, isoamyl nitrite, DME, reflux, 4 h; 2) aqueous NaOH, MeOH, 55% (**3**), 45% (**4**). See the Supporting Information for details.

With respect to the earlier experiments with R = H, Me and CMe_3 we observed a drastic increase in the *syn*/*anti* ratio of the triptycene product with R = $SiMe_3$. Instead of 0:100 for R = CMe_3, we now observe a strong preference for the *syn*-isomer (for R = $SiMe_3$ *syn*/*anti* mixture 84:16). A similar observation was made with R = $GeMe_3$, but the preference for the *syn*-isomer was less pronounced (*syn*/*anti* mixture 70:30). As both, Si and Ge, are more electropositive atoms than carbon, the original prediction by the calculations seemed to have proven true, and even the higher electronegativity of germanium compared to silicon seems to be reflected in the experimental results. Comparable results—a favored formation of *syn*-Diels–Alder cycloaddition products—are observed when, for example, $SiMe_3$- instead of CMe_3-substituted furane derivatives are converted with haloarynes.[19]

The isomers in the product mixtures of **3** and **4** could be separated by sublimation and were characterized by ^1H, $^{13}C\{^1H\}$, and $^{29}Si\{^1H\}$ NMR spectroscopy as well as high-resolution mass spectrometry. In the case of *anti*-**3**, the rotation about the C_{Ar}–Si axis is found to be hindered, as is indicated by two resonances at 0.99 (6H) and 0.55 ppm (3H), induced by the protons of the $SiMe_3$ substituent. A similar splitting has been observed earlier for the *tert*-butyl analogue of *anti*-**4**.[12] Characteristic for the two different isomers, *syn* and *anti*, are the singlet resonances of the bridgehead proton H9. That of *syn*-isomer (*syn*-**4**) experiences a larger downfield shift than that of the *anti*-isomer (*anti*-**4**) (δ = 7.12 vs. 6.49 ppm).

The molecular structures of *syn*-**3** and *syn*-**4**, as determined by single-crystal X-ray diffraction,[20] are shown in Figure 1. Both compounds are isostructural. The molecules are of C_3 symmetry (close to C_{3v}) and exhibit paddlewheel configurations. Benzene and methyl substituents are arranged in a staggered conformation. The C–C bonds in the benzene rings vary by about 0.03 Å in length around that of benzene (1.395 Å[21]). Longer are the distances C(2)–C(3) and C(4)–C(5) [1.517(2), 1.548(2) Å (*syn*-**3**); 1.519(2), 1.545(2) Å (*syn*-**4**)]. The bonds C(4)–E(1) are significantly elongated compared to the corresponding standard $C(sp^3)$–E distances [1.922(2) Å (*syn*-**3**) vs. 1.87 Å and

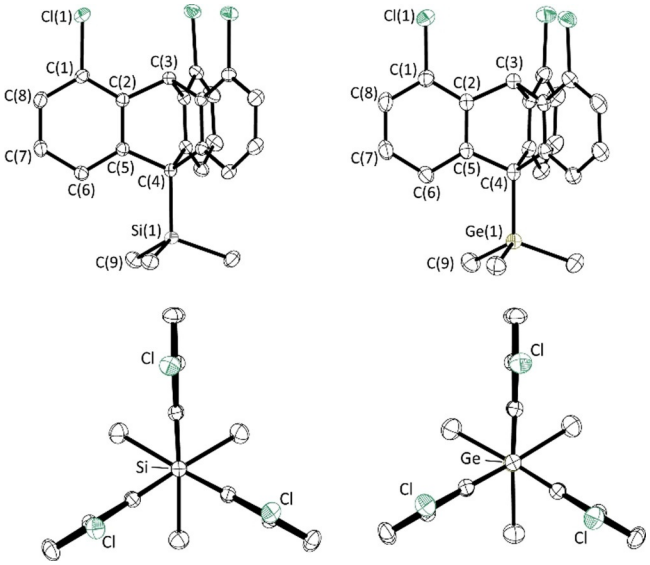

Figure 1. Molecular structures of *syn*-**3** and *syn*-**4** in the crystal. Side views (above) and views along the C(3)–C(4)–E(1) axis (below). Displacement ellipsoids are drawn at 50% probability level. Hydrogen atoms are omitted for clarity. Selected bond lengths [Å] and angles [°] for *syn*-**3**/*syn*-**4**: C(1)–C(2) 1.386(2)/1.382(2), C(1)–C(8) 1.393(2)/1.399(3), C(1)–Cl(1) 1.744(1)/1.742(2), C(2)–C(3) 1.517(1)/1.519(2), C(2)–C(5) 1.408(1)/1.402(2), C(4)–C(5) 1.548(1)/1.545(2), C(4)–E(1) 1.922(2)/1.994(3), C(9)–E(1) 1.879(1)/1.954(2), Cl(1)–C(1)–C(2) 119.8(1)/120.0(1), Cl(1)–C(1)–C(8) 118.9(1)/118.9(1), C(1)–C(2)–C(3) 126.4(1)/126.6(2), C(2)–C(1)–C(8) 121.2(1)/121.0(2), C(2)–C(3)–C(2′) 105.6(1)/105.5(1), C(3)–C(2)–C(5) 113.8(1)/113.8(2), C(4)–C(5)–C(6) 127.2(1)/126.8(2), C(5)–C(4)–E(1) 114.2(1)/114.0(1).

1.994(3) Å (*syn*-**4**) vs. 1.96 Å].[22] This indicates intramolecular repulsion between the hydrogen atoms at C(6) and the methyl groups.

The fact that electronic parameters dominate the regioselectivity of the reactions combined with the inability of charges to predict the reaction prompted us to gain a more detailed view of this aryne [4+2] cycloaddition reaction. The most direct way of theoretical investigation of reactions and their product distribution is the calculation of structures and energies of the corresponding transition states. We performed such calculations for a series of reactions by using different approximations. To establish a benchmark and to find the most suitable level of theory, we calculated the barriers of activation for the simplest system first: the reaction of 1,8-dichloroanthracene with chlorobenzyne (for details, see Table S4). It turned out that the best and still affordable method is DFT using the B3LYP functional with the 6-31G(d,p) basis set including corrections for basis-set superposition error. The optimized transition-state structures are shown in Figure 2.

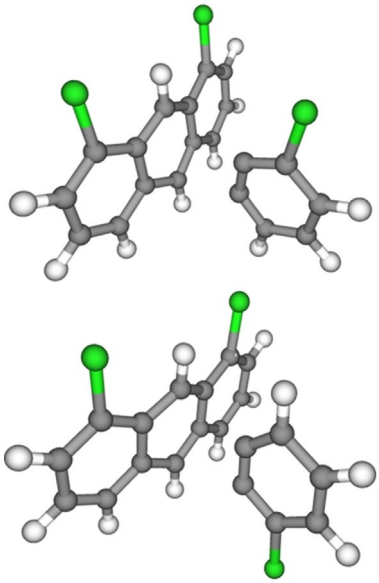

Figure 2. Optimized [B3LYP/6-31G(d,p)] transition-state structures for the formation reaction of 1,8,13-trichlorotriptycene (*syn*, above) and 1,8,16-trichlorotriptycene (*anti*, below).

AIM and interacting quantum atoms (IQA) techniques[23] revealed interesting aspects for these transition-state structures (Figures S4 and S5). Bond critical points (BCP) appear during bond formation in the reactions, with their properties being those of weakly stabilizing closed-shell interactions. Natural energy decomposition analysis (NEDA) in NBO theory[24] shows better stabilization for the transition states of *anti*-trichlorotriptycene than for the *syn*-isomer (Table S6). The lower activation barrier makes *anti*-trichlorotriptycene the preferred product in the corresponding reaction. Detailed analysis reveals the importance of the electronic component (sum of electrostatic, polarization, and self-energies) in this better stabilization. Relating the relative energies for the transition states for *syn*- and *anti*-isomers to the corresponding experimentally observed *syn*/*anti* product ratios in reactions of chlorobenzyne with 1,8-dichloroanthracene (Table 1), the B3LYP/6-31G(d,p) results so far supported at least qualitatively the observations.

Table 1. Results of the trichlorotriptycene syntheses by conversion of the corresponding 1,8-dichloroanthracene derivatives **1** and **2** with in situ-generated chloroaryne. The data for other 10-substituted 1,8-dichloroanthracenes (R-10 = CMe_3, Me, H) are given for comparison.[12] The reactions have been also investigated by quantum-chemical calculations (see the main text and the Supporting Information). All yields are given for isolated mixtures of *syn*- and *anti*-trichlorotriptycenes.

Compound	R-10	*Syn* [%]	*Anti* [%]	Yield [%]	Product
	H	21	79	16	
	Me	37	63	42	
	CMe_3	0	100	43	
1	$SiMe_3$	84	16	55	**3**
2	$GeMe_3$	70	30	45	**4**

However, we could not achieve even a qualitatively correct prediction of the product ratio for the reaction with R = $SiMe_3$ (Scheme 2). Consequently, a substantial series of additional calculations was performed (Table S7) to find more reliable transition-state energies for this reaction. All attempts of expanding the basis set, using different DFT functionals and modeling in solution, did not improve the calculated energies: the barriers to the formation of the *syn*-isomer (with R = $SiMe_3$) were still predicted higher than those for the corresponding *anti*-isomer. Attempts to account for static correlation with the CASSCF method did either not give results compatible with the experimental findings. However, single-point MP2[25] and XMCQDPT2 energies[26] for the transition-state structures from the respective RHF and CASSCF calculations indicated that dynamic correlation plays a significant role in these reactions. To test this hypothesis further, we carried out very time-consuming MP2/def2-SV(P) optimizations for the transition states. These revealed that the transition states for the formation of *syn*- and *anti*-trichloro-10-(trimethylsilyl)triptycene (**3**) can have completely different structures (Figure 3: TS to the *syn*-isomer) to those predicted by DFT calculations. The validity of this transi-

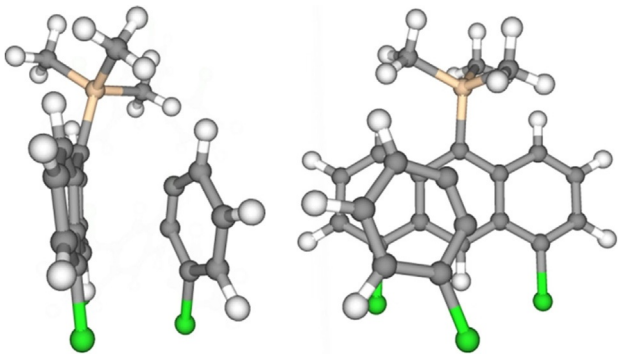

Figure 3. Different views of the optimized [MP2/def2-SV(P)] transition-state structure of the formation of *syn*-1,8,13-trichloro-10-(trimethylsilyl)triptycene (*syn*-**3**).

tion-state structure for the *syn*-isomer on this particular level of theory has been verified by computing the full reaction path.

Figure 3 shows the structure of the transition state of the reaction of **1** with chloroaryne to *syn*-1,8,13-trichloro-10-(trimethylsilyl)triptycene (**3**). Surprisingly, we see that it is likely stabilized by π-stacking of the benzyne ring with the anthracene molecule. Unfortunately, all our attempts to find computationally and to fully prove the existence of a transition state to the *anti*-isomer of **3** were not successful.

Despite its seeming simplicity, the formation of triptycenes from the reaction of arynes with anthracenes turns out to be a highly complex system governed by many parameters that require a subtle balance. The finding of a distinct contribution of dispersion in the transition state sheds new light on such reactions. We will now examine further tailor-made reference systems experimentally and theoretically in order to gain an increasingly valid description of the multiple factors that determine the regioselectivity of such reactions.

Acknowledgements

This work was supported by Deutsche Forschungsgemeinschaft [DFG, Priority Program SPP 1807 "Control of London dispersion interactions in molecular chemistry" (MI477/28-1)]. We thank Klaus-Peter Mester for recording NMR spectra, Heinz-Werner Patruck for measuring mass spectra, Regionales Rechenzentrum Köln (RRZK) for providing computing time (supercomputer CHEOPS), and Johanna Grote for designing the graphical abstract layout. We also acknowledge support for the Article Processing Charge from the DFG and the Open Access Publication Fund of Bielefeld University.

Conflict of Interest

The authors declare no conflict of interest.

Keywords: anthracenes · cycloaddition · dispersion · solid-state structures · triptycenes

[1] P. D. Bartlett, M. J. Ryan, S. G. Cohen, *J. Am. Chem. Soc.* **1942**, *64*, 2649 – 2653.
[2] G. Wittig, R. Ludwig, *Angew. Chem.* **1956**, *68*, 40.
[3] T. M. Swager, *Acc. Chem. Res.* **2008**, *41*, 1181 – 1189.
[4] J. H. Chong, M. J. MacLachlan, *Chem. Soc. Rev.* **2009**, *38*, 3301 – 3315.
[5] C.-F. Chen, *Chem. Commun.* **2011**, *47*, 1674 – 1688.
[6] For example, a) V. E. Williams, T. M. Swager, *Macromolecules* **2000**, *33*, 4069 – 4073; b) Z. Zhu, T. M. Swager, *J. Am. Chem. Soc.* **2002**, *124*, 9670 – 9671; c) J. Hoogboom, T. M. Swager, *J. Am. Chem. Soc.* **2006**, *128*, 15058 – 15059; d) D. Maag, T. Kottke, M. Schulte, A. Godt, *J. Org. Chem.* **2009**, *74*, 7733 – 7742.
[7] C. Azerraf, S. Cohen, D. Gelman, *Inorg. Chem.* **2006**, *45*, 7010 – 7017.
[8] a) K. Nikitin, H. Müller-Bunz, Y. Ortin, J. Muldoon, M. J. McGlinchey, *J. Am. Chem. Soc.* **2010**, *132*, 17617 – 17622; b) D. K. Frantz, A. Linden, K. M. Baldridge, J. S. Siegel, *J. Am. Chem. Soc.* **2012**, *134*, 1528 – 1535.
[9] J.-S. Yang, C.-P. Liu, B.-C. Lin, C.-W. Tu, H.-G. Lee, *J. Org. Chem.* **2002**, *67*, 7343 – 7354.
[10] For more and detailed insights in (tr-)iptycenes and their applications see: a) Y. Jiang, C.-F. Chen, *Eur. J. Org. Chem.* **2011**, 6377 – 6403; b) C.-F. Chen, Y.-X. Ma, *Iptycenes Chemistry—From Syntheses to Applications, 1st ed.*, Springer-Verlag, Berlin, **2012**; and the references cited therein.
[11] a) M. Mastalerz, I. M. Oppel, *Angew. Chem. Int. Ed.* **2012**, *51*, 5252 – 5255; *Angew. Chem.* **2012**, *124*, 5345 – 5348; b) M. W. Schneider, H.-J. S. Hauswald, R. Stoll, M. Mastalerz, *Chem. Commun.* **2012**, *48*, 9861 – 9863; c) G. Zhang, O. Presly, F. White, I. M. Oppel, M. Mastalerz, *Angew. Chem. Int. Ed.* **2014**, *53*, 5126 – 5130; *Angew. Chem.* **2014**, *126*, 5226 – 5230; d) S. M. Elbert, F. Rominger, M. Mastalerz, *Chem. Eur. J.* **2014**, *20*, 16707 – 16720; e) G. Zhang, O. Presly, F. White, I. M. Oppel, M. Mastalerz, *Angew. Chem. Int. Ed.* **2014**, *53*, 1516 – 1520; *Angew. Chem.* **2014**, *126*, 1542 – 1546; f) E. H. Menke, V. Lami, Y. Vaynzof, M. Mastalerz, *Chem. Commun.* **2016**, *52*, 1048 – 1051.
[12] a) J. Chmiel, I. Heesemann, A. Mix, B. Neumann, H.-G. Stammler, N. W. Mitzel, *Eur. J. Org. Chem.* **2010**, 3897 – 3907; b) J. Chmiel, Dissertation, Westfälische Wilhelms-Universität Münster, **2010**.
[13] a) J. Chmiel, B. Neumann, H.-G. Stammler, N. W. Mitzel, *Chem. Eur. J.* **2010**, *16*, 11906 – 11914; b) J.-H. Lamm, J. Horstmann, J. H. Nissen, J.-H. Weddeling, B. Neumann, H.-G. Stammler, N. W. Mitzel, *Eur. J. Inorg. Chem.* **2014**, 4294 – 4301; c) J.-H. Lamm, P. Niermeier, A. Mix, J. Chmiel, B. Neumann, H.-G. Stammler, N. W. Mitzel, *Angew. Chem. Int. Ed.* **2014**, *53*, 7938 – 7942; *Angew. Chem.* **2014**, *126*, 8072 – 8076; d) J.-H. Lamm, J. Glatthor, J.-H. Weddeling, A. Mix, J. Chmiel, B. Neumann, H.-G. Stammler, N. W. Mitzel, *Org. Biomol. Chem.* **2014**, *12*, 7355 – 7365; e) J. Horstmann, M. Hyseni, A. Mix, B. Neumann, H.-G. Stammler, N. W. Mitzel, *Angew. Chem. Int. Ed.* **2017**, *56*, 6107 – 6111; *Angew. Chem.* **2017**, *129*, 6203 – 6207.
[14] M. E. Rogers, B. A. Averill, *J. Org. Chem.* **1986**, *51*, 3308 – 3314.
[15] J. M. Medina, J. L. Mackey, N. K. Garg, K. N. Houk, *J. Am. Chem. Soc.* **2014**, *136*, 15798 – 15805.
[16] J. P. Foster, F. Weinhold, *J. Am. Chem. Soc.* **1980**, *102*, 7211 – 7218.
[17] R. F. W. Bader, *Atoms in Molecules—A Quantum Theory*, University Press, Oxford, **1990**.
[18] J.-H. Lamm, Yu. V. Vishnevskiy, E. Ziemann, T. A. Kinder, B. Neumann, H.-G. Stammler, N. W. Mitzel, *Eur. J. Inorg. Chem.* **2014**, 941 – 947.
[19] a) G. W. Gribble, D. J. Keavy, S. E. Branz, W. J. Kelley, M. A. Pals, *Tetrahedron Lett.* **1988**, *29*, 6227 – 6230; b) E. Masson, M. Schlosser, *Eur. J. Org. Chem.* **2005**, 4401 – 4405.
[20] CCDC 1002356 and 10023567 contain the supplementary crystallographic data for syn-**3** and syn-**4**, respectively. These data are provided free of charge by The Cambridge Crystallographic Data Centre.
[21] J. Clayden, N. Greeves, S. Warren, *Organische Chemie, 2nd. ed.*, Springer-Verlag, Berlin, **2013**.
[22] B. Cordero, V. Gómez, A. E. Platero-Prats, M. Revés, J. Echeverría, E. Cremades, F. Barragán, S. Alvarez, *Dalton Trans.* **2008**, 2832 – 2838.
[23] M. A. Blanco, A. Martín Pendás, E. Francisco, *J. Chem. Theory Comput.* **2005**, *1*, 1096 – 1109.
[24] a) E. D. Glendening, A. Streitwieser, Jr., *J. Chem. Phys.* **1994**, *100*, 2900 – 2909; b) G. K. Schenter, E. D. Glendening, *J. Phys. Chem.* **1996**, *100*, 17152 – 17156; c) E. D. Glendening, *J. Am. Chem. Soc.* **1996**, *118*, 2473 – 2482.
[25] C. Møller, M. S. Plesset, *Phys. Rev.* **1934**, *46*, 618 – 622.
[26] A. A. Granovsky, *J. Chem. Phys.* **2011**, *134*, 214113.

Received: December 8, 2017

